MODELING STRONG EFFECTS OF ROTATING SYSTEM IN THE COMPUTATION OF TURBULENT FLOWS IN CHANNELS

E. M. Smirnov and A. V. Shatrov

UDC 532.517.4

In the analysis of the effect of rotation on turbulent flow in channels whose center line is perpendicular to the axis of rotation it is necessary to differentiate direct effects due to nonconservative Coriolis force on the generation (source) of turbulent energy and changes in turbulence characteristics caused by the restructuring of the flow field by the mean velocity, i.e., indirect effects. Effects of the first group are observed in the "pure" form in the flow along plane parallel channel whose walls are parallel to the axis of rotation [1]. Various attempts to model these effects are considered in [2, 3]. Effects of the second group are fundamental in the flow through channels with the dominating role played by walls normal to the axis of rotation.

The global restructuring of the mean velocity field caused by rotation, which involves the production of the core of the flow with homogeneous velocity distribution along lines parallel to the axis of rotation, and formation of thin wall layers, leads to strong variations in turbulence characteristics [4, 5]. As indicated by experimental data on the drag coefficient [4, 5], rotation at a certain high speed can even lead to laminarization of an initially turbulent flow. With further increase in the angular speed, a rapid increase in pressure loss is observed (almost proportional to $\omega^{1/2}$). In particular, in the case of flows through the cooling ducts of the rotors of powerful motors, it is this aspect of the effect of the Coriolis force on turbulent flow that appears to be most important. Conditions under which Coriolis forces disturb the flow are studied with numerical modeling in [6, 7]. Results of numerical modeling are presented below for the simplified representation of strong effects of rotation caused by restructuring of the mean velocity field, including laminarization.

1. Consider incompressible flow through a prismatic slot-shaped channel, whose long, parallel sides are at a distance 2h apart. The channel rotates at a constant angular speed ω about an axis perpendicular to the channel walls. The role of the short side walls in the formulation of the problem is to determine the direction of the total mass transfer.

We introduce Cartesian coordinates fixed to the channel and oriented such that the y axis is along the axis of rotation, the z axis is parallel to the channel walls in the flow direction, and the origin is located at the midplane of the channel. Assuming that the mean flow is steady and fully developed along the streamwise coordinate z, we neglect the end effects at bounding side walls. Thus the velocity field and turbulence characteristics are assumed to depend only on the transverse coordinate y.

Introducing modified pressure $p^* = (\langle p\rangle/\rho) - (1/2)\omega^2 r^2$ (r is the shortest distance to the axis of rotation), and taking the above assumptions into consideration, we write Reynolds equations

$$\frac{d}{dy}\left(\nu\frac{dU}{dy} - \langle uv\rangle\right) = \frac{\partial p^*}{\partial x} + 2\omega W, \quad \frac{d}{dy}\left(\nu\frac{dW}{dy} - \langle wv\rangle\right) = \frac{\partial p^*}{\partial z} - 2\omega U, \tag{1.1}$$

with boundary conditions

$$U = W = 0 \quad \text{at} \quad y = \pm h \tag{1.2}$$

and integral relations

$$\int_{-h}^{h} W\,dy = 2hW_m, \quad \int_{-h}^{h} U\,dy = 0, \tag{1.3}$$

whose first equation reflects constant mass flow in the direction of z (W_m = const is the mean flow rate) while the second equation is the result of no-slip conditions at the side walls of the channel.

Leningrad. Translated from Zhurnal Prikladnoi Mekhaniki i Tekhnicheskoi Fiziki, No. 5, pp. 35-41, September-October, 1985. Original article submitted December 27, 1983.

0021-8944/85/2605-0635$09.50

It is seen that the quantity p* should be a linear function of coordinates x, z, i.e., p* = Ax + Bz + C, where A, B, and C are constants.

The closure of the problem is achieved by assuming the scalar nature of the turbulent eddy viscosity coefficient ν_t

$$-\langle uv\rangle = \nu_t \frac{dU}{dy}, \quad -\langle wv\rangle = \nu_t \frac{dW}{dy} \tag{1.4}$$

and we use the (k − ε) model of turbulence [8] which is suitable for the computation of flows with low turbulent Reynolds numbers (k is the turbulent kinetic energy and ε is its rate of dissipation).

In the present problem the Coriolis body force vector lies in the plane perpendicular to the direction of velocity displacement. Analysis of the differential equations for Reynolds stresses shows that in the given situation there is no basis to expect appreciable direct effects due to rotation on turbulent transfer. In any case, errors arising from the negligence of direct effects are of the same order as that introduced by the assumption of the scalar nature of the quantity ν_t. In this sense, the present flow is similar to the flow on a rotating disk. Approbation of the (k − ε) model in computing the flow around a rotating disk [9] may be considered extremely successful. The above-mentioned conditions and conclusions [10] relative to the values of empirical constants determined the use of (k − ε) model [8] in the same form

$$\frac{d}{dy}\left[(\nu+\nu_t)\frac{dk}{dy}\right] = -P+\varepsilon+2\nu\left(\frac{dk^{1/2}}{dy}\right)^2,$$

$$\frac{d}{dy}\left[\left(\nu+\frac{\nu_t}{\sigma_\varepsilon}\right)\frac{d\varepsilon}{dy}\right] = -c_1\frac{\varepsilon P}{k}+c_2 f_\mu\frac{\varepsilon^2}{k}-c_3 G_\mu;$$

$$P = \nu_t\left[\left(\frac{dU}{dy}\right)^2+\left(\frac{dW}{dy}\right)^2\right],$$

$$G_\mu = \nu\nu_t\left\{\frac{d}{dy}\left[\left(\frac{dU}{dy}\right)^2+\left(\frac{dW}{dy}\right)^2\right]^{1/2}\right\}^2, \tag{1.5}$$

$$\nu_t = c_4\exp[-2{,}5/(1+\mathrm{Re}_t/50)]\frac{k^2}{\varepsilon},$$

$$f_\mu = 1{,}0-0{,}3\exp(-\mathrm{Re}_t^2), \quad \mathrm{Re}_t = \frac{k^2}{\nu\varepsilon},$$

$$c_1 = 1.55,\ c_2 = 2{,}0,\ c_3 = 2{,}0,\ c_4 = 0{,}09,\ \sigma_\varepsilon = 1{,}3,$$

$$k = 0,\ \varepsilon = 0 \ \text{ at } \ y = \pm h.$$

As an example of flow characteristics we choose Reynolds number $\mathrm{Re} = 2W_m h/\nu$ and $\gamma = \omega h^2/\nu$. We introduce the nondimensional coordinate $\eta = y/h$ and in discussing results of the solution to the problem (1.1)-(1.5) we keep in view flow symmetry relative to the plane y = 0.

2. Integration of a nonlinear system of differential equations for U, W, k, and ε was carried out numerically using a conservative finite-difference scheme with nonuniform grid [11]. Concentration of grid points near the wall was achieved using the geometric progression

$$\xi_m = \xi_1\frac{1-q^{m-1}}{1-q}, \quad \xi_1 = \frac{1-q}{1-q^{M-1}}, \quad m = \overline{2, M},$$

where $\xi = 1-\eta$; M is the number of grid points in the interval $0 \leqslant \xi \leqslant 1$.

Relaxation technique was used to obtain the stationary solution. The fictitious time-interval τ_m was changed from grid point to grid point in proportion to the local interval in time $\tau_m = \alpha(\xi_{m+1}-\xi_m)$, while the relaxation process remained unchanged.

The method used to linearize equations for k and ε determines, to a large extent, the permissible time interval, in particular the factor α. Systematic computations showed the effectiveness of using the following linearization:

$$\frac{k_n-k_{n+1}}{\tau_m}+\frac{d}{dy}\left[(\nu+\nu_t)_n\frac{dk_{n+1}}{dy}\right]+P_n-\frac{\varepsilon_n k_{n+1}}{k_n} = 2\nu\left(\frac{dk_n^{1/2}}{dy}\right)^2,$$

$$\frac{\varepsilon_n-\varepsilon_{n+1}}{\tau_m}+\frac{d}{dy}\left[\left(\nu+\frac{\nu_t}{\sigma_\varepsilon}\right)_n\frac{d\varepsilon_{n+1}}{dy}\right]+c_1\frac{P_n\varepsilon_n}{k_n}-c_2 f_\mu\frac{\varepsilon_n\varepsilon_{n+1}}{k_n} = -c_3(G_\mu)_n.$$

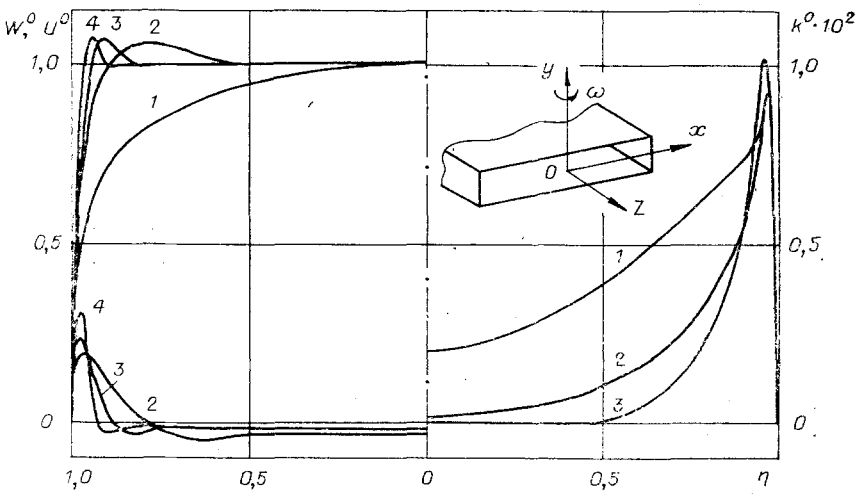

Fig. 1

At each new (n + 1) time-interval the system of algebraic equations for $k_{n+1,m}$ and $\varepsilon_{n+1,m}$ were solved using a shooting technique for scalar equations and the system for $U_{n+1,m}$ and $W_{n+1,m}$ was solved simultaneously with shooting technique for three-point vector equations.

Prandtl's hypothesis was used to determine the initial distribution for $W_0(y)$. The mixing length l was given by the Prandtl–Nikuradze relation with van Driest correction [12]. It was assumed that $U_0(y) = 0$. Initial distributions for k_0 and ε_0 were determined using the Townsend equation

$$k_0(y) = -c_0 \langle wv \rangle = c_0 l^2 (dW/dy)^2, \; c_0 = 10/3$$

and assuming local equilibrium in turbulence $\varepsilon_0 = P_0(y)$. The initial distributions thus determined approximately describe the fields W, k, and ε in the turbulent flow along a fixed plane plane-parallel channel.

Basic computations were carried out with M = 51 (q = 1.1) and M = 101 (q = 1.04). Laminar flow in a slot-like channel whose analytical solution is known [13], and computed results for turbulent flow in a fixed channel [8, 14] using the same turbulence model, were used as test cases. Practically coincident results were obtained in all cases.

3. The effect of rotation on the same velocity field and turbulent energy is illustrated in Fig. 1, where Re = 30,400, curves 1-4 correspond to γ = 0; 1000; 2000; and 2500. The streamwise velocity component W_c at the center section was used as the reference. The velocity profile $W^0(\eta) = W(\eta)/W_c$ gets fuller with an increase in rotational speed. The flow is divided into a core with uniform velocity distribution and a shear layer near the wall called the Ekman layer. The circulation in the transverse direction initially increases with γ, attains a maximum, and then decreases as in the case of laminar flow [13], whereas, during this process, the function $\Phi(\gamma) = \max\{U^0(\eta)\}$ is monotonic.

The major content in the transformation of the k^0 field is the production of fluctuating flow in the core. It is important to mention that the level of turbulent kinetic energy in the wall layer undergoes a relatively small change. A sharp, almost catastropic reduction in k^0 right up to zero is observed in this region only at a certain high speed (γ = 2500). Thus, the combination Re = 30,400 and γ = 2500 is an example of the flow condition when the initially introduced fluctuation in the flow model is fully degenerated in the settling process.

The distributions of the nondimensional eddy viscosity coefficient $\nu_t^0 = \nu_t/\nu$ and the quantity $l^0 = c^{3/4}k^{3/2}/\varepsilon h$ characterizing turbulence scale are shown in Fig. 2 for the same pair Re, γ. A reduction in the characteristic shear layer thickness, naturally, leads to a reduction in the scale of energy-containing vortices. The latter also causes a sharp drop in ν_t^0 with an increase in γ, in spite of a weak change in fluctuations in the wall layer.

The distributions of nondimensional velocity components determined with the use of wall layer scales are shown in Fig. 3 (the notation is the same as in Fig. 1), where $w_* = V_* \times \sqrt{\cos\alpha_*}$, $u_* = V_*\sqrt{\sin\alpha_*}$, $V_* = \sqrt{\tau^*/\rho}$, τ^* is the modulus of total shear stress at the wall, $\alpha_* = \arctan(\tau_x^*/\tau_z^*)$, $\xi_* = \xi V_*/\nu$.

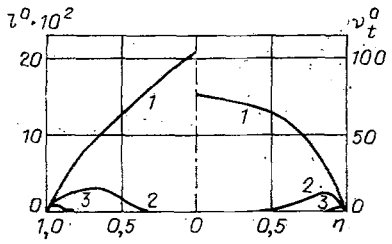

Fig. 2

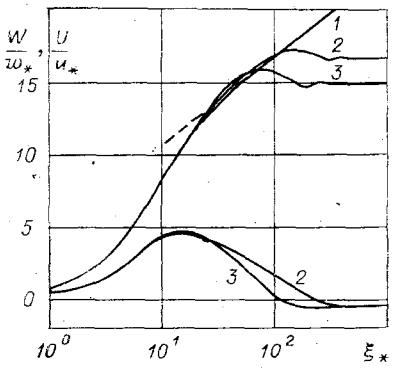

Fig. 3

The dependence of W/w_* on ξ_*, even at very high rotational speeds, has regions close to the "universal" logarithmic law (dashed line) for the two-dimensional boundary layer. We also note that the maximum in the $U(\xi_*)/u_*$ profile is located in the transition region from the viscous sublayer to the turbulent region.

4. A large number of computed variants was used to determine the relation between the coefficient of resistance of the rotating channel

$$\lambda = -\frac{4h}{W_m^2}\frac{\partial p^*}{\partial z}$$

and the parameters Re and γ (Fig. 4, curves 1-5 correspond to γ = 0; 500; 1000; 2000; and 4000). The dashed line extension to the curve 1 has been plotted according to [8]. The straight line 6 corresponds to resistance law in plane-parallel fixed channel flow with a laminar regime ($\lambda = 24/\mathrm{Re}$). The branches of curves 2-5 for laminar and turbulent flows are conditionally connected by dashed lines. The determination of converging solution in these ranges of Re is difficult and the narrowing of the uncertainty interval is associated with large computational time.

It is not possible to carry out a direct verification of the adequacy of the present turbulence model because of the absence of experimental data on the characteristics of fully developed flow as well as on pressure losses in a slot-shaped channel with the present orientation. However, comparison with results [4] from square channel is in favor of the model. Through an analysis of experimentally determined relations for the coefficient of resistance, an attempt was made in [4] to determine the zone of transition on the Re, $K = 4\gamma/\mathrm{Re}$ plane to turbulent flow in the rotating channel. The error in the data obtained for critical values of Re_* is about 30% when K = const. Points on the error bound region in Re_* are shown in Fig. 4 where the black symbols indicate the lower bounds and the open symbols are for higher bounds. Such a good agreement between computed and experimental data on the determination of the influence of rotation on laminar–turbulent transition can be considered remarkable with reference to the difference in geometric forms. It is worth keeping in view, however, that the sharp variation in the relations $\lambda(\mathrm{Re}, \gamma = \mathrm{const})$ or $\lambda(\mathrm{Re}, K = \mathrm{const})$ for rapidly rotating square channels is due to the very turbulization of the near-wall Ekman layers at the surfaces perpendicular to the axis of rotation. The last statement is based on the realization of the crucial contribution made by these layers to the total surface resistance. Thus, from the point of view of the determination of pressure loss, it is possible to consider the flow in a square channel ($2h \times 2h$) as a part of a slot-type channel with length 2h along the x axis. With such an approach, the results of the comparison made in Fig. 4 do not appear to be so unexpected.

5. The results of the present problem could be used for the practical estimation of secondary flows in the core of the flow and for the determination of the limits of applicability of the technique to divide the flow into the core and the near-wall Ekman layer, which makes it possible to develop effective approximate solutions to more complex internal flow problems involving rotating systems. The near-wall shear layer thickness is characterized by two quantities, the first one δ_1 being determined by the condition $|W/W_c - 1| \leqslant 0.01$ for $(h - y) > \delta_1$, and the second δ_2 is equal to the distance from the wall to the point at which the transverse velocity component changes sign. We also introduce mass flow circulating in the direction of x axis,

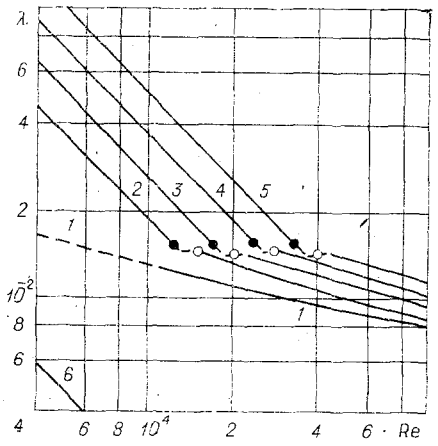

Fig. 4

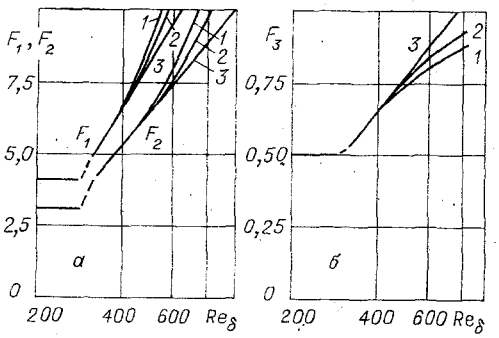

Fig. 5

$$q = \int_{h-\delta_2}^{h} Udy = -\int_{0}^{h-\delta_2} Udy$$

and nondimensionalize thicknesses δ_1 and δ_2 with respect to the thickness [15] of the linear Ekman layer $\delta = \sqrt{\nu/\omega}$ and the quantity q with respect to $W_c\delta$.

It is expedient to use the quantity $Re_\delta = W_c/\sqrt{\nu\omega}$ as the reference parameter of the flow in the near-wall layers. Actually, when $\gamma \to \infty$, Re/γ = const the characteristic thickness of the Ekman layer decreases monotonically ($\delta_{1,2}/h \to 0$), the velocity W_c tends to the mean flow value W_m, and the quantity h drops out of the characteristic flow parameters in the layer. The remaining quantities ν, ω, $W_c \to W_m$ may be used to obtain a unique nondimensional combination Re_δ. In the general case, when the quantity γ is not very large, we should write

$$\delta_1/\delta = F_1(Re_\delta, \gamma),\ \delta_2/\delta = F_2(Re_\delta, \gamma),\ q/(W_c\,\delta) = F_3(Re_\delta, \gamma).$$

The relation between the functions F_i (i = 1, 2, 3) and Re_δ, γ is shown in Fig. 5; for the curves 1-3, γ = 1000, 2000, and 4000. When $Re_\delta \lesssim 300$, F_i is constant, which corresponds to laminar flow in the Ekman layer. After a break at $Re_\delta \simeq 300$, indicating transition to turbulent flow, the quantity F_i monotonically increases with Re_δ. It is interesting that at γ = 4000 in the computed range of Re_δ, the quantity $F_i \sim \ln Re_\delta$.

The relation $q/(h - \delta_2)W_c = F_3/(\gamma^{1/2} - F_2)$ could be considered an estimate of the strength of the secondary flow in the core for the given γ and Re_δ $Re/2\gamma^{1/2}$.

LITERATURE CITED

1. J. P. Johnston, R. M. Halleen, and D. K. Lezius, "Effects of spanwise rotation on the structure of two dimensional fully turbulent channel flow," J. Fluid Mech., 56, Pt. 3 (1972).
2. J. H. G. Howard, S. V. Patankar, and R. M. Bordynuik, "Flow prediction in rotating ducts using Coriolis-modified turbulence models," Trans. ASME, J. Fluid Eng., 102, 456 (1980).
3. C. Hah, "Turbulence closure and prediction of the wake in a rotating wall shear layer," AIAA J., 20, No. 11 (1982).
4. E. Dobner, "Über den Strömungswiderstand in einem rotierenden Kanal," Diss., Technische Hochschule, Darmstadt (1959).
5. M. Piesche, "Experimente zum Strömungswiderstand in gekrümmten rotierenden Kanälen mit quadratischen Querschnitt," Acta Mech., 42 (1982), p. 145.
6. A. K. Majumdar, V. S. Pratap, and D. B. Spalding, "Numerical computation of flow in rotating ducts," Trans. ASME, Basic Eng., 99, 148 (1977).
7. R. Simon, R. Schilling, and K. O. Felsch, "Berechnung der ausgebildeten turbulenten Strömung in rotierenden Kanälen mit rechteckigem Querschnitt," Strömungsmech. Strömungsmasch., No. 28 (1980).
8. W. P. Jones and B. E. Launder, "The prediction of laminarization with two-equations model of turbulence," Int. J. Heat Mass Transfer, 15, 301 (1972).
9. B. E. Launder and B. I. Sharma, "Application of the energy-dissipation model of turbulence to flow near a spinning disk," Lett. Heat Mass Transfer, 1, No. 2 (1974).

10. B. E. Launder, C. H. Priddin, and B. I. Sharma, "The calculation of turbulent boundary layers on spinning and curved surfaces," Trans. ASME, J. Basic Eng., 99, No. 1 (1977).
11. A. A. Samarskii, Theory of Difference Methods [in Russian], Nauka, Moscow (1977).
12. K. K. Fedyaevskii, A. S. Ginevskii, and A. V. Kolesnikov, Computation of Incompressible Turbulent Boundary Layer [in Russian], Sudostroenie, Leningrad (1973).
13. O. N. Ovchinnikov and E. M. Smirnov, "Dynamics of flow and heat transfer in rotating slot-type channel," Inzh. Fiz. Zh., 35, No. 1 (1978).
14. K.-Y. Chien, "Predictions of channel and boundary-layer flows with a low-Reynolds-number turbulence model," AIAA J., 20, No. 1 (1982).
15. Kh. Greenspan, Theory of Rotating Fluids [in Russian], Gidrometeoizdat, Leningrad (1975).

FLOW OVER LAMBDA WINGS WITH FLAPS

O. N. Ivanov and A. I. Shvets

UDC 533.6.011.55+629.782.015.3

Flow over wings of lambda-shaped cross section and over star-shaped bodies has been investigated in [1-5].

For control of an aircraft in the cruise regime and also for takeoff and landing one must have mechanical devices such as flaps. Their effectiveness depends considerably on boundary layer separation. Separation on two-dimensional and axisymmetric bodies, and also three-dimensional separation in flow over obstacles have been studied in a number of papers, but as yet limited data are available on boundary layer separation on triangular wings with flaps [6]. No data have as yet been published on lambda wings with flaps.

The flow and boundary layer separation on lambda-shaped wings with flaps have been investigated in a supersonic wind tunnel at $M = 0.3$-3 and $Re_c = (1\text{-}3)\cdot 10^6$. We tested three models of triangular lambda wings with vertex angles $\Lambda = 180$, 160, 121° and sweepback angle in the wing plane of $\chi = 71°$ (Fig. 1). For all three models the flap slope angle was $\delta = 0$ and 40°, and for the model with vertex angle $\Lambda = 161°$ we also tested at $\delta = 21°$. The wing span for all three models was $R = 140$ mm, and the thickness was 10 mm. The wing leading edges were made sharp, with a wedge angle of $\beta = 25°$, to obtain an attached shock wave at $M = 3$. The models were attached to the α-mechanism by means of a rear sting with $d = 28$ mm and $l = 200$ mm, in the form of a half cylinder with a wedge cutaway ($\psi = 20°$) along the central chord of the leeward side of the lambda wing. The pressure at points on the model surface with coordinates s along the central chord $c = 200$ mm was measured with an induction sensor, with the aid of a pressure commutator. The relative error of pressure measurement was ±2%. The oil film method was used to investigate the stream lines and the separation boundaries on the surface of the wing and the flap.

We shall examine the influence of the vertex angle Λ (Fig. 1a, $\alpha = 15°$, $M = 3$, $\delta = 40°$, points 1-3 refer to $\Lambda = 180$, 161, 120°) and the flap deflection angle δ (Fig. 1b, $\alpha = 15°$, $M = 3$, $\Lambda = 161°$, points 4-6 refer to $\delta = 0$, 21, 40°) on the pressure distribution and the location of the separation point. The pressure distribution curves on the lambda wings and in the plane of the triangular wing ($\Lambda = 180°$) are similar, while the pressure on the flap continues to increase as the angle Λ is reduced. It was established from the pressure measurements of [6] that the nature of the pressure distribution changes very little over the span of a plane triangular wing, in spite of the flow being three-dimensional in this zone. However, the pressure on the flap varies appreciably over its span because of the intense spreading of the flow, and the maximum pressure is found in the central part. The vertex angle $\Lambda = 161°$ is close to the optimal angle of $\Lambda = 150°$ to certain the maximum lift-to-drag ratio in the class of equivalent wings [4]. On this lambda wing model we studied the flow for three values of the flap deflection angle ($\delta = 0$, 21, 40°) (see Fig. 1b). The flap deflection at angle $\delta = 21°$ for $\alpha = 0$ gives a sharp pressure increase only on the flap, and at $\alpha = 15°$ in the immediate vicinity of the wing-flap discontinuity ($s/c = -0.025$) (see Fig. 1b), which agrees with the results of [6], where nonseparated flow was found at hypersonic speeds for a plane triangular wing with flap deflection angles $\delta \leqslant 20°$. In addition, for this flap we

Moscow. Translated from Zhurnal Prikladnoi Mekhaniki i Tekhnicheskoi Fiziki, No. 5, pp. 41-46, September-October, 1985. Original article submitted June 15, 1984.

 0021-8944/85/2605-0640$09.50